Effect of local environment on nanoscale dynamics at electrochemical interfaces: Anisotropic growth and dissolution in the presence of a step providing evidence for a Schwoebel–Ehrlich barrier at solid/liquid interfaces

Yufan He and Eric Borguet*

Department of Chemistry and Surface Science Center, University of Pittsburgh, Pittsburgh, PA, 15260, USA. E-mail: borguet@pitt.edu

Received 11th November 2001, Accepted 14th January 2002
First published as an Advance Article on the web 7th May 2002

The dynamics of nanoscale islands in the vicinity of a monoatomic step on a metal electrode surface under potential control have been investigated by potential pulse perturbation time-resolved scanning tunneling microscopy (P^3 TR-STM). As the metastable islands decay, a clear anisotropy develops in the spatial distribution of islands, relative to the monoatomic step. Islands appear to be stabilized above the step, while a denuded region develops below the step over a distance of about 100 nm. Vacancy islands are observed to be more stable than adatom islands. These results provide evidence for an electrochemical Schwoebel–Ehrlich barrier to diffusion of atoms across the step.

Introduction

Steps have long been postulated to play an important role in the mechanisms of thin film growth and surface catalysis.[1,2] The presence of steps is a basic factor, with kinetic as well thermodynamic consequences, that affects the surface morphology resulting from thin film growth and the rates of surface catalyzed chemical reactions.[1,2] Steps are known to affect diffusion dynamics and are cited as the source of discrepancy between macroscopic and microscopic diffusion experiments.[3] Attachment and detachment from kinks in steps are postulated as the fundamental events in crystal growth and dissolution processes.[4] STM and atomic force microscopy (AFM) are in many respects ideal probes of surface dynamics and have enabled considerable progress in understanding the role of steps on dynamics in ultra high vacuum (UHV).[5,6] There has, however, been less progress on the effect of steps on surface dynamics in other environments, *e.g.*, electrochemical.[7,8] This is important as it is not obvious that UHV concepts will transfer to other environments.

The kinetics of island decay in the vicinity of steps on metal surfaces in UHV has been the focus of recent interest[9–13] and some controversy.[14,15] A frequently invoked explanation for the difference in the observed island decay rates above and below a step is the Schwoebel–Ehrlich (S–E) barrier. The S–E barrier, first described over 30 years ago, is a barrier to atoms crossing a step from one terrace to the next (Scheme 1), either above or below it.[16,17] Early UHV field ion microscope experiments revealed that, contrary to prevailing notions of the time, adatoms from the two sides of a step do not incorporate into the step with equal probability.[16] The S–E barrier is frequently revealed by a capture anisotropy, a difference in the probability of incorporation of an adatom when approaching the step from above *versus* approach from below.

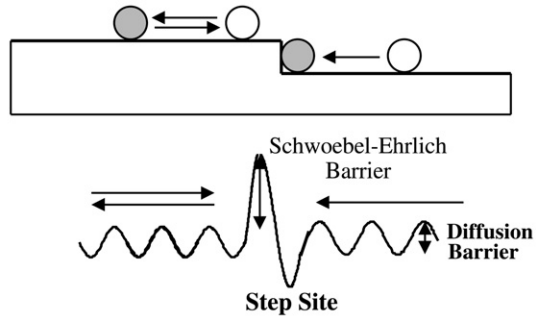

Scheme 1

The physical origin of the Schwoebel–Ehrlich barrier is still controversial.[18] The simplest picture, which associates the barrier with a loss of coordination of the atom rolling over the step edge, is not consistent with all the observations, namely the order of magnitude difference in the S–E barriers for A and B types steps on Pt(111).[18] However, Feibelman argues that the lowest barrier, downward-transport mechanism proceeds via a concerted substitution.[19] The difference in the barriers for A and B steps is related to the coordination of the transition state.[19] The higher S–E barrier B step is associated with a lower, threefold coordination transition state than the A step whose transition state is fourfold coordinated.[19]

The role of steps and associated S–E barriers in the development of surface morphology arises from the requirement of interlayer transport for effective layer by layer growth.[9,20,21] Atoms must be able to cross steps for smooth surfaces to grow. The persistence of small vacancy islands or holes in the surface is taken as evidence for a S–E barrier to hopping of adatoms over a descending step.[9] Further evidence for a S–E barrier is provided by the widening of an island free zone at the ascending step with the simultaneous absence of such a zone at a descending step. This provides evidence for accelerated decay of an island at an ascending step.[9]

The Au(111) surface provides a convenient means to generate a low density of islands in an electrochemical environment.[22] The Au(111) surface has two stable phases; the unreconstructed (1×1) and the reconstructed $(22 \times \sqrt{3})$.[23] At room temperature in UHV, the $(22 \times \sqrt{3})$ phase is the stable phase.[24] In an electrochemical environment, a transition between the two phases can be induced by changing the electrode potential, first suggested by classical voltammetry.[25] The reconstruction has been investigated by a number of techniques including second harmonic generation,[26–28] surface X-ray scattering,[29] and STM.[22,30–33] It is now well established that the reconstructed Au(111)-$(22 \times \sqrt{3})$ surface transforms to the Au(111)-(1×1) phase at potentials above ~440 mV *vs.* SCE, and that the reverse transition occurs for potentials below ~220 mV *vs.* SCE in $HClO_4$ solution.[31] The density of the reconstructed phase is estimated to be about 4.5% higher than that of the unreconstructed phase.[30]

The dynamics of the phase transitions of Au(111) in electrolyte have been reported and shown to depend on the potential at which the transition occurs.[31] However, there has been to our knowledge no report of the effect of steps on the dynamics or resultant surface morphology. While the S–E barrier has been invoked in electrochemistry,[34,35] we are not aware of any previous report of direct evidence, *e.g.* STM images, revealing an S–E barrier in environments other than UHV. It is not *a priori* obvious that phenomena, such as the S–E barrier, observed in UHV should have counterparts at liquid/solid interfaces. There are a number of surfaces, *e.g.*, Cu(100), for which no apparent S–E barrier was detected in UHV.[36] In addition, the S–E barrier has been connected with surface states.[18] Our results are not consistent with models that connect the S–E barrier with surface states,[11] as these are believed to be quenched at liquid/solid interfaces such as the electrochemical interfaces investigated here.

We report experiments revealing that island decay rates are highly correlated to the position of the islands relative to steps in an electrochemical environment. This result suggests the existence of a "Schwoebel–Ehrlich" barrier in an electrochemical environment, *i.e.*, a barrier to diffusion across a step.[16,17]

Experimental

The substrate, an Au(111) single crystal (Monocrystals Co., Ohio) was cleaned by immersion in hot piranha solution (1 : 3 H_2O_2 and H_2SO_4) for 1 h, and immersion in hot HNO_3 for 30 min. After each step the sample was rinsed by ultrasonication in ultrapure water (> 18 MΩcm). (**Caution! The piranha solution is a very strong oxidizing agent and extremely dangerous to handle in the laboratory. Protective equipment including gloves, goggles and face shields should be used at all times.**) The crystal was hydrogen flame annealed, and allowed to cool to room temperature in air. The sample was transferred to the STM electrochemical cell and immersed under potential control (0.1 V *vs.* SCE) in 0.1 M $HClO_4$ solution. The sample was occasionally electropolished at 3 V potential in 1 M H_2SO_4 solution.[37] All electrode potentials are quoted relative to the SCE potential (V *vs.* SCE).

STM images were obtained with a PicoScan STM system (Molecular Imaging) with a bi-potentiostat to control the sample and tip potential independently. The electrochemical cell was made of Teflon. A silver wire and a platinum wire were used as a quasi-reference electrode and counter electrode, respectively. All cell components were chemically cleaned in the same way as the crystal. STM tips were prepared by electrochemically etching 0.25 mm diameter tungsten wires using 10 V AC, in 3M KOH solution. Tips, coated with paraffin wax, yielded less than 10 pA Faradaic current. All the STM images were obtained under constant current mode at 0.5 nA, −0.15 V tip-sample bias. All the images were scanned from bottom to top. This direction also serves as a time axis. Each image was acquired in about 100 s.

The time constant of the electrode–electrolyte system is short. Even with pulses as rapid as 0.1 s, a very rapid lifting of the reconstruction is observed. This suggests a time constant significantly less than 1 s.[22] No evidence for tip-assisted dynamics, or mechanical contact with the surface, was observed in our experiments. In several instances we have zoomed out to explore a larger area and seen no apparent differences between the smaller repeatedly scanned area and the larger area that surrounded it.

P^3 TR-STM has been described previously.[22] Briefly, the STM monitors the evolution of the sample morphology, on a frame by frame basis, after a short positive potential pulse. After the perturbing pulse, the sample returns to its initial potential.

Results and discussion

At low potentials, thermodynamically favoring the reconstructed phase, the characteristic herringbone pattern is observed.[22,23,25,26,29–31,33] Higher resolution images typically showed the characteristic herringbone pattern of the reconstructed surface.[22,31,32] A single monatomic step traverses the middle of the image taken prior to application of the potential pulse perturbation (Fig. 1A). The top right-hand corner of Fig. 1A shows three closely bunched monoatomic steps, separated by terraces less than 15 nm wide.

When the potential was stepped rapidly to 0.7 V *vs.* SCE for 10 s the reconstruction was rapidly lifted to yield the less dense (1×1) phase.[22] The lifting of the reconstruction appeared to be complete as the characteristic herringbone pattern of reconstructed stripes disappeared entirely, and islands appeared.[22] Fig. 1B shows the surface covered with islands immediately after the pulse was applied. The size and distribution of the islands were initially the same above and below the step. However, the surface morphology changed with time, as can be qualitatively recognized by comparing the bottom of the image with the top portion of the image, representative of the surface at longer times after the perturbing pulse, as well by inspection of successive images (Fig. 1B–E).

Three distinct phenomena were observed. First, both the island size and density evolved with time. For example, the bottom of Fig. 1B shows a large number of small islands, whereas at the top of the image, recorded at longer time after the pulse, the islands were larger and their density, *i.e.*, the number of islands per unit area, was smaller. As time evolved, the STM images (Fig. 1B–E) show that the number of islands had further reduced, and their average size had increased.

The islands disappeared because they were metastable at this potential (0.1 V *vs.* SCE).[22] It should be noted that not all islands disappeared, similar to our recent observations of Au islands on Au(111) in an electrochemical environment.[22] The development of the island distribution shows evidence of Ostwald ripening.[9] Large islands appeared to grow at the expense of smaller islands, a consequence of the Gibbs–Thompson effect.[38] Perimeter atoms evaporate from small islands faster

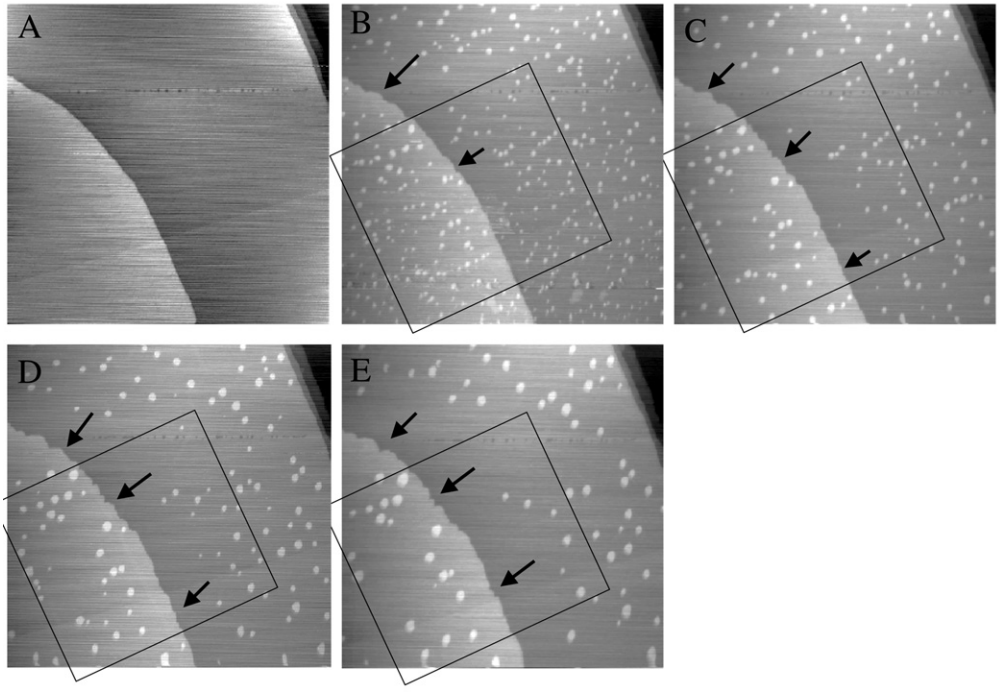

Fig. 1 STM image (487 nm × 487 nm) of Au(111)/0.1 M $HClO_4$ at 0.1 V *vs.* SCE (vertical scale 10 Å). (A) Prior to potential pulse perturbation, (B) 0–108, (C) 109–219, (D) 220–320, (E) 456–556 s after a 10 s, 0.7 V *vs.* SCE pulse. Images are scanned from bottom to top.

than from large islands. Hence, at a constant rate of capture of "evaporated" atoms by small and large islands, the latter experience a net flow of material from the former.

Second, a clear anisotropy in the distribution of islands with respect to location relative to the step, developed with time. In contrast to the surface imaged directly after the pulse (Fig. 1B), the surface shown in Fig. 1E showed a clear anisotropy in the island distribution with respect to the step. A denuded zone, which appeared to contain no islands, developed below the step. This region grew to about 100 nm wide in Fig. 1E. Above the step, however, islands persisted even quite close to the step. Indeed these islands appeared, for the most part, to have grown in the time that elapsed between the acquisition of images shown in Fig. 1B and Fig. 1E.

Third, the morphology of the step changed. The initially, relatively uniform step edge developed some kinks, indicated by arrows in Fig. 1A–D, as time elapsed. This change seems to have resulted from the incorporation of atoms released by island decay.

In order to quantitatively characterize the effect of the step on island decay, a rectangular area (328×298 nm^2) was chosen, in which the terrace area above and below the step are about equal. In the absence of any influence on the step, the island decay dynamics should be similar on the terrace above the step and the terrace below the step. The effect of the step on island decay dynamics can be investigated by comparing the evolution of the island distribution and total island area on both terraces.

The time dependence of the total island area on the terrace below and above the step, depicted in Fig. 2, shows that the islands decayed much faster on the terrace below the step than on the terrace above the step. Two possible processes may decrease the total island area: (1) the phase transition from the unreconstructed Au(111)-(1×1) to the reconstructed $(22 \times \sqrt{3})$ surface; (2) atom detachment, diffusion and incorporation into the step. The decrease in island area resulting from the consumption of atoms to enable the phase transition from the (1×1) to the denser $(22 \times \sqrt{3})$ surface should have a similar rate above and below the step. Thus, the greater rate of total island area decrease for the terrace below the step, as opposed to the terrace above the step, results from

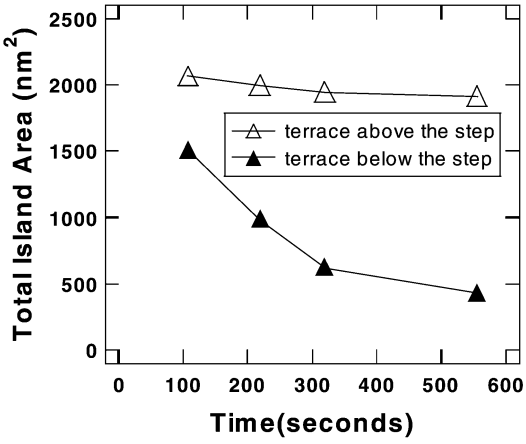

Fig. 2 Time dependence of the total island area on the terrace below the step (▲) and above the step (△) in the box shown in Fig. 1. The total area in the box is about 328×298 nm^2. The initial island decay rate is about 5 atoms s^{-1} above the step, and 38 atoms s^{-1} below the step.

atoms that detach from islands, diffuse and incorporate into the step. This result suggests that the ascending step can accelerate the decay of the islands and that the step may be a sink for atoms that approach it from below.

The histograms of distance from the island center to the step at different times, Fig. 3B–E, show the time dependence of the island distribution on the terrace below and above the step. On the terrace above the step, the distribution of islands was quite uniform shortly after the perturbing voltage pulse. As time elapsed, the islands did not decay uniformly. Islands far from the descending step decayed faster, resulting in the distribution shifting toward the step. However, on the terrace below the step, the result is the opposite, islands near the step decayed faster than islands far from the step, resulting in the development of a denuded zone containing no islands in the vicinity of the ascending step. Hence, the island distribution shifted away from the ascending step. This result shows that the ascending step affects the island distribution quite differently from the descending step. This result suggests that below the step, atoms from islands near the ascending step can readily detach, diffuse and incorporate to the ascending step. However, above the step, the adatoms cannot descend to the step and accordingly accumulate in the vicinity of the step. Accordingly, we conclude that the atoms attaching to the step come from islands on the terrace below the step and not from the terrace above the step. These results provide evidence for the effect of local environment on the island decay rate.

The islands in the vicinity of a descending step are much more stable than those in the vicinity of an ascending step. This is also apparent from inspection of Fig. 1, where the remaining islands (Fig. 1E) appear to cluster near the step in the middle and in the top right-hand corner of the image. Indeed, the descending step appears to retard the decay of the islands in its vicinity, resulting in the enhanced stability of islands near the steps. The apparent enhanced stability near a descending step can be understood as a consequence of the nearly perfectly reflecting nature of the S–E barrier for an atom approaching the descending step (Scheme 1). The flux of atoms leaving an island towards the descending step is almost exactly balanced by a flux of atoms reflected by the barrier at the descending step. This observation is consistent with the slower rate of decay of total island area on the upper terrace (Fig. 2).

The effect of local environment on the island decay rate is usually thought to be one of the characteristics of diffusion limited decay.[9] In the diffusion limit, mass transport is determined by gradients in the adatom density on the terraces between island edges, or step edges in general.[38] In fact, the step can be thought of as a very large island. The line tension associated with the step is thus much smaller than that of the small islands. In the vicinity of the ascending step, there is a large gradient in the adatom density between the island edge and the step. Therefore, atom diffusion toward the ascending step and incorporation into the ascending step are much faster than

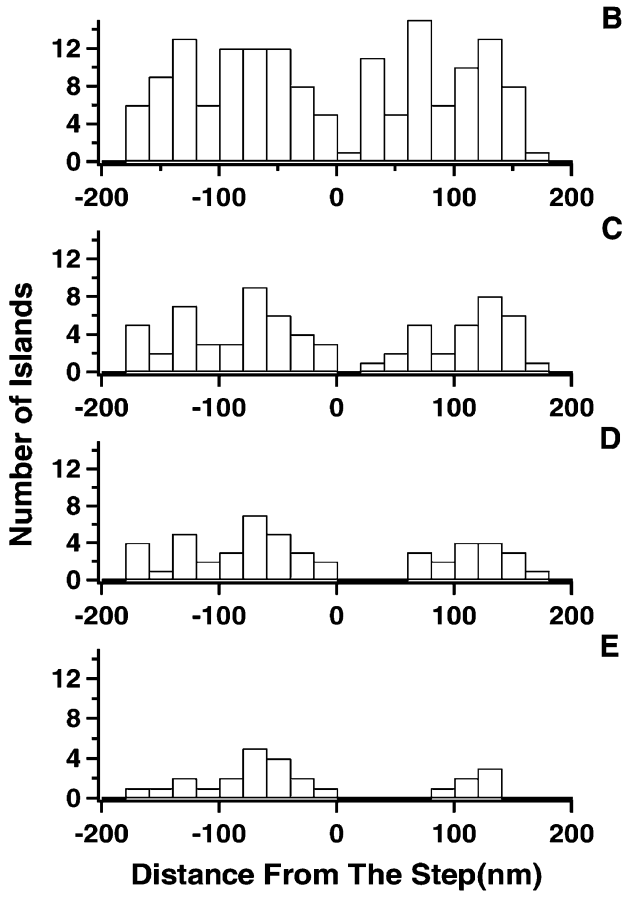

Fig. 3 Histograms of the time dependence of the island distance distribution in the box shown in Fig. 1(B)–(E). The distance from the step to the islands is set to be negative on the terrace above the step and positive for islands on the terrace below the step.

from an ascending step to an island or from one island to another island of similar size. This is one of the reasons why the island decay is accelerated in the vicinity of the ascending step.

At this potential (0.1 V *vs.* SCE), the unreconstructed Au(111)-(1×1) phase is not stable. It tends to convert into the more stable reconstructed Au(111) phase. In addition, because of line tension, the nanoscale islands are metastable, and they tend to ripen into large islands so that the fraction of edge atoms of these islands is minimized. Accordingly, two mechanisms are present in this island decay process. (1) Small islands decay to provide atoms to the phase transition from (1×1) to $(22 \times \sqrt{3})$. (2) Atoms detach from island edges, diffuse and incorporate to the edge of big islands or ascending steps. These are competitive processes. If the phase transition from (1×1) to $(22 \times \sqrt{3})$ is fast, the adatoms from the decay of small islands will diffuse and incorporate into the substrate to form the reconstructed structure. In this case, Ostwald ripening will not be apparent as larger islands will not grow. However, if the phase transition from (1×1) to $(22 \times \sqrt{3})$ is slow, the decay of small islands can provide more adatoms than needed by the phase transition. Then, diffusing adatoms can attach to island perimeters and incorporate into the islands, causing the larger islands to grow, revealing Ostwald ripening.

The island area distribution evolves differently, after the perturbing pulse, on the terrace above and below the step (Fig. 1). The histogram of the island area distribution at different times after the perturbing pulse on the terraces above and below the step is shown in Fig. 4. On the terrace above the step, the number of islands decreases, and the center of the area distribution of islands shifts

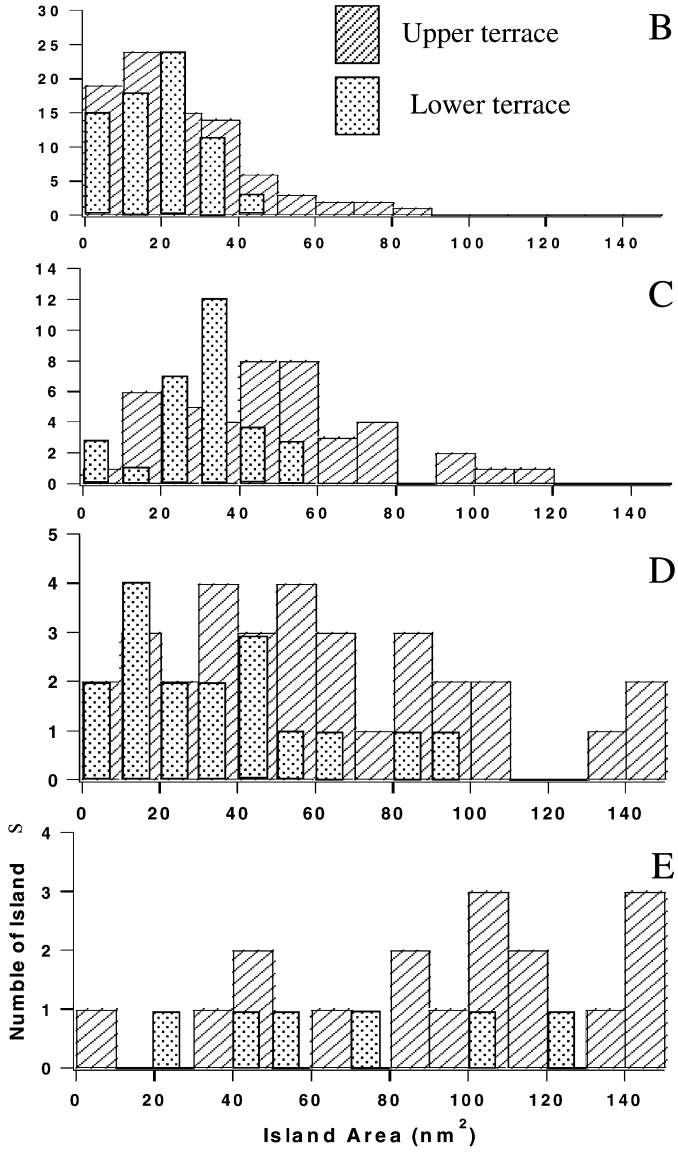

Fig. 4 Histograms of the time dependence of the island area distribution in the box shown in Fig. 1(B)–(E).

towards increasing island size, indicating that small islands decay, and that large islands grow, indicative of Ostwald ripening. This result suggests that the phase transition from (1×1) to $(22 \times \sqrt{3})$ is a slower process than island decay, and is not limited by atoms detaching from small islands. However, on the terrace below the step, although the average island area increases, more islands have disappeared and only a few islands remain. In the vicinity of the ascending step, atoms tend to diffuse toward the step and incorporate into the step. This process is faster than atom detachment from the island perimeter. Therefore, all islands, no matter how small or large, decay to release adatoms. These atoms diffuse and incorporate into the ascending step, consequently, leading to the formation of an island free region.

Another interesting observation, consistent with the existence of a S–E barrier, was that vacancy islands appeared to be much more stable than adatom islands. A linear cluster of vacancies,

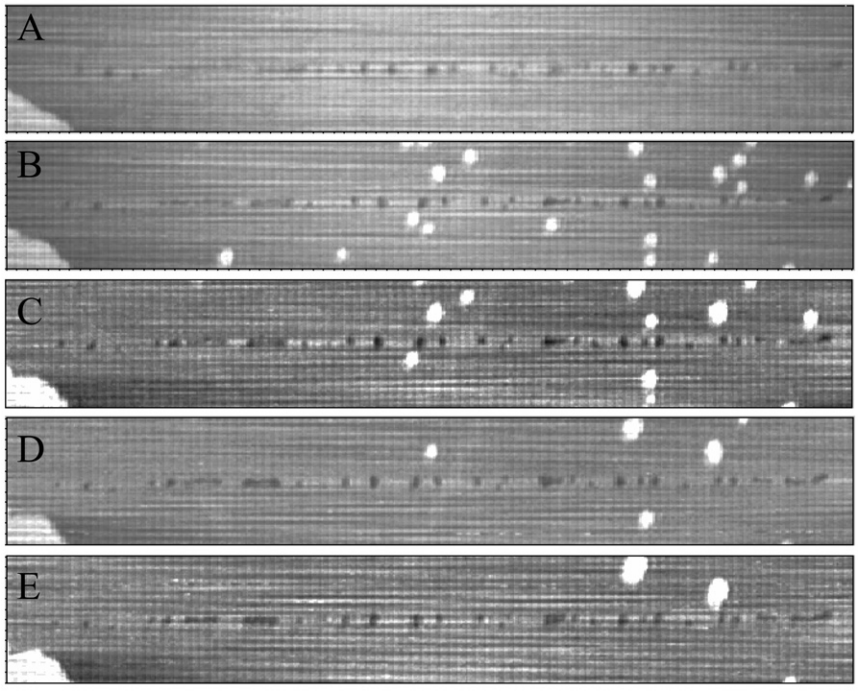

Fig. 5 STM image (60 nm × 400 nm) of Au(111)/0.1 M $HClO_4$ at 0.1 V *vs.* SCE (vertical scale 3 Å). These images are enlargements of a section in the upper half of the images shown in Fig. 1, The acquisition time of each image is about 13 s. (A) Prior to potential pulse perturbation, (B) 73–87, (C) 181–195, (D) 287–290, (E) 523–536 s after a 10 s pulse to 0.7 V *vs.* SCE.

apparent in the upper half of Fig. 1 prior to the P^3 sequence, is shown in a magnified image (Fig. 5A). Interestingly, the perturbation did not appear to modify the vacancy islands significantly (Fig. 5B). The vacancy islands did not appear to grow or diffuse. Atoms detaching from the perimeter of adatom islands in close proximity to vacancy islands did not seem to fill the vacancy islands, presumably because of the S–E barrier to atoms crossing a descending step from the terrace into the vacancy island (Fig. 5C–5E). A similar observation was noted for vacancy islands on Ag(111) at room temperature under UHV.[39] The evident stability of these vacancy islands provides further, independent proof for a S–E barrier at electrochemical interfaces.

Conclusion

Our experimental observations support the existence of a "Schwoebel–Ehrlich" barrier on a metal surface under electrochemical conditions. The evidence for this barrier is provided by the widening of an island free zone at the ascending step with the simultaneous absence of such a zone at a descending step. We also see evidence for stability of vacancy islands consistent with the observation of a Schwoebel–Ehrlich barrier. These results provide strong evidence for accelerated decay of islands at an ascending step. In addition, the retarded decay of islands at a descending step is noted. These observations open the way for studies of the effect of potential on the Schwoebel–Ehrlich barrier.

Acknowledgement

The authors acknowledge the generous support of the NSF and Research Corporation. EB acknowledges the NSF for a CAREER award (CHE-9734273) and the Research Corporation for a Research Innovations Award in support of this research.

References

1 G. A. Somorjai, *Introduction to Surface Chemistry and Catalysis*, Wiley, New York, 1994.
2 H. Brune, *Surf. Sci. Rep.*, 1998, **31**, 125.
3 J. V. Barth, *Surf. Sci. Rep.*, 2000, **40**, 75.
4 I. N. Stranski, *Z. Phys. Chem.*, 1928, **136**, 259.
5 S. Baier and M. Giesen, *Phys. Chem. Chem. Phys.*, 2000, **2**, 3675.
6 O. M. Magnussen and M. R. Vogt, *Phys. Rev. Lett.*, 2000, **85**, 357.
7 A. A. Gewirth and B. K. Niece, *Chem. Rev.*, 1997, **97**, 1129.
8 R. M. Nyffenegger and R. M. Penner, *Chem. Rev.*, 1997, **97**, 1195.
9 G. S. Icking-Konert, M. Giesen and H. Ibach, *Surf. Sci.*, 1998, **398**, 37.
10 M. Giesen, G. S. Icking-Konert and H. Ibach, *Phys. Rev. Lett.*, 1998, **80**, 552.
11 M. Giesen, G. S. Icking-Konert and H. Ibach, *Phys. Rev. Lett.*, 1999, **82**, 3101.
12 M. Giesen and H. Ibach, *Surf. Sci.*, 2000, **464**, L697.
13 K. Morgenstern, G. Rosenfeld and G. Comsa *et al.*, *Phys. Rev. B*, 2001, **63**, 5412.
14 K. Morgenstern, G. Rosenfeld and G. Comsa *et al.*, *Phys. Rev. Lett.*, 2000, **85**, 468.
15 M. Giesen and H. Ibach, *Phys. Rev. Lett.*, 2000, **85**, 469.
16 G. Ehrlich and F. G. Hudda, *J. Chem. Phys.*, 1966, **44**.
17 R. L. Schwoebel, *J. Appl. Phys.*, 1969, **40**.
18 M. Giesen, *Prog. Surf. Sci.*, 2001, **68**, 1.
19 P. J. Feibelman, *Phys. Rev. Lett.*, 1998, **81**, 168.
20 A. F. Becker, G. Rosenfeld and B. Polesma *et al.*, *Phys. Rev. Lett.*, 1993, **70**, 477.
21 H. A. vanderVegt, H. M. vanPinxteren and M. Lohmeier *et al.*, *Phys. Rev. Lett.*, 1992, **68**, 3335.
22 Y. He and E. Borguet, *J. Phys. Chem. B*, 2001, **105**, 3981.
23 D. M. Kolb, *Prog. Surf. Sci.*, 1996, **51**, 109.
24 K. G. Huang, D. Gibbs and D. M. Zehner *et al.*, *Phys. Rev. Lett.*, 1990, **65**, 3313.
25 D. M. Kolb and J. Schneider, *Electrochim. Acta*, 1986, **31**, 929.
26 A. Friedrich, B. Pettinger and D. M. Kolb *et al.*, *Chem. Phys. Lett.*, 1989, **163**, 123.
27 G. Luepke, G. Marowsky and R. Steinhoff, *Phys. Rev. B*, 1990, **41**, 6913.
28 A. Friedrich, C. Shannon and B. Pettinger, *Surf. Sci.*, 1991, **251–252**, 587.
29 J. Wang, B. M. Ocko and A. J. Davenport *et al.*, *Phys. Rev. B*, 1992, **46**, 10321.
30 X. Gao, A. Hamelin and M. J. Weaver, *J. Chem. Phys.*, 1991, **95**, 6993.
31 N. J. Tao and S. M. Lindsay, *Surf. Sci. Lett.*, 1992, **274**, L546.
32 N. J. Tao and S. M. Lindsay, *J. Appl. Phys.*, 1992, **70**, 5141.
33 D. M. Kolb, A. S. Dakkouri, N. Batina, in *Nanoscale Probes of the Solid/Liquid Interface*, ed. A. A. Gewirth and H. Siengenthaler, Kluwer, Dordrecht, 1995, vol. 288, p. 263.
34 R. McHardy, W. H. Haiss and R. J. Nichols, *Phys. Chem. Chem. Phys.*, 2000, **2**, 1439.
35 M. I. Haftel and T. L. Einstein, *Appl. Surf. Sci.*, 2001, **175**, 49.
36 J. B. Hannon, C. Klünker and M. Giesen *et al.*, *Phys. Rev. Lett.*, 1997, **79**, 2506.
37 J. L. Whitton and J. A. Davies, *J. Electrochem. Soc.*, 1964, **111**, 1347.
38 G. Rosenfeld, K. Morgenstern and I. Beckmann *et al.*, *Surf. Sci.*, 1998, **404**, 401.
39 K. Morgenstern, G. Rosenfeld and G. Comsa, *Phys. Rev. Lett.*, 1996, **76**, 2113.